Specification and Performance Analysis of Wi-SUN FAN

REI HIRAKAWA [ID]**, KEIICHI MIZUTANI** [ID] **(Member, IEEE), AND HIROSHI HARADA** [ID] **(Senior Member, IEEE)**

Graduate School of Informatics, Kyoto University, Kyoto 606-8501, Japan

CORRESPONDING AUTHOR: HIROSHI HARADA (e-mail: hiroshi.harada@i.kyoto-u.ac.jp)

ABSTRACT In recent years, extensive research has been conducted on the Internet of Things (IoT). Wireless
Smart Ubiquitous Network (Wi-SUN) has gained considerable attention as a wireless communication stan-
dard for IoT. Wi-SUN Field Area Network (Wi-SUN FAN) is a technical specification of Wi-SUN that can be
implemented in both indoor and outdoor IoT communication infrastructure with multi-hop routing. Although
Wi-SUN FAN version 1.0 (Wi-SUN FAN 1.0) has been standardized by IEEE 2857–2021, there have been no
studies or reviews conducted on the transmission performance of Wi-SUN FAN 1.0 regarding transmission
success rate and delay time using computer simulations and experimental evaluation environments involving
actual devices. In this study, the specifications of the Wi-SUN FAN are reviewed, and the fundamental
transmission performance, such as average transmission success rate and average delay time, is measured
using computer simulation as reference data. An experimental evaluation environment involving actual
devices is developed to validate the characteristics evaluated by computer simulation. The characteristics
determined by the computer simulation and experimental evaluation environment are in good agreement.
Using the validated simulator, we evaluate the transmission performance in the wireless IoT environment
with one border router and 100 routers randomly arranged in a flat square field with 4,000 m on a side. The
average transmission success rate is approximately 1 at 1.00×10^{-1} s^{-1} or less. Consequently, Wi-SUN
FAN 1.0 can communicate with a higher transmission success rate even when transmitting frequent IoT-data,
which is once every ten seconds.

INDEX TERMS IEEE 2857, IEEE 802.15.4, multihop, RPL, Wi-SUN FAN.

I. INTRODUCTION

The research and development (R&D), demonstration test-
ing, and commercialization of the Internet of Things (IoT)
have been conducted extensively in recent years. IoT involves
wireless devices equipped with various "things", including
sensors, meters, and monitors. The information collected from
the physical space is transmitted into a cyberspace comprising
data management servers and databases, and new applications
are created by linking the collected data with other data [1],
[2]. The Wireless Smart Ubiquitous Network (Wi-SUN) is
a wireless communication standard for IoT [2], [3], [4], [5],
[6], [7]. Wi-SUN employs a physical layer compliant with
IEEE 802.15.4–2015 [4], [8], an international standard for
low data rates and low-power consumption. It primarily uses
a frequency lower than 1 GHz band, which is called sub-1

GHz, and can transmit over a long distance of several hundred
meters to one kilometer at a power of approximately 20 mW
[2] or higher. Furthermore, the Carrier Sense Multiple Access
with Collision Avoidance (CSMA/CA) standardized in IEEE
802 15.4–2015 is adopted as the datalink layer protocol to re-
duce the radio interference between the radio nodes within the
same frequency [2]. Wi-SUN has developed several technical
specifications called profiles in Wi-SUN Alliance to flexibly
support various applications. The typical profiles include the
Wi-SUN Home Area Network (HAN) and Wi-SUN Field
Area Network (FAN) [7].

Wi-SUN HAN consists of two types of communication,
as shown in Fig. 1(a). The first is direct communication
between the electricity smart meter and Home Energy Man-
agement System (HEMS). The second is point-to-multipoint
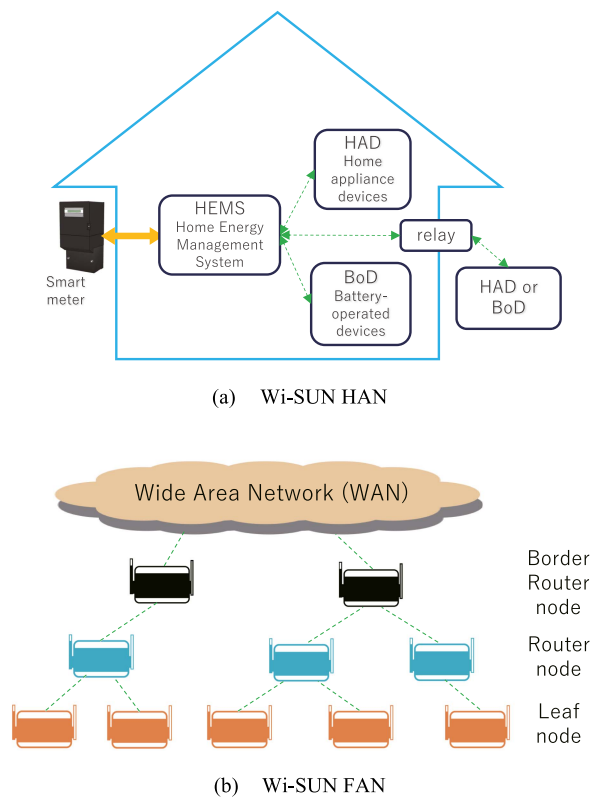
(a)   Wi-SUN HAN

(b)   Wi-SUN FAN

FIGURE 1. Wi-SUN application.

communication between the HEMS and various devices, such as home appliances, solar panels, storage batteries, etc. In Japan, the Wi-SUN HAN is widely adopted as a communication method between the electricity smart meter and HEMS, and more than 10 million smart meters with the function of Wi-SUN HAN have already been introduced [9]. Moreover, the FAN connecting smart meters outdoors achieves a connection rate of 99.6%, assuming power measurements that transmit packets once every 30 minutes or so [9].

Wi-SUN FAN is a communication specification used to transmit data acquired from outdoor-installed sensors, meters, and monitors to the cloud and control these devices using the cloud based on the analysis results of the collected data, as illustrated in Fig. 1(b). In May 2016, Wi-SUN Alliance standardized the technical communication specification as Wi-SUN FAN 1.0 [7], and the Wi-SUN FAN 1.0 was also standardized as IEEE 2857 in June 2021 [10]. FSK is adopted as a transmission scheme for physical layers with data rates of 50, 100, and 150 kbps in Wi-SUN FAN 1.0 by using frequency bands in the sub-1 GHz range. Furthermore, Wi-SUN FAN adopts frequency hopping (FH) along with CSMA/CA to avoid interference in communication among different nodes. The network layer of Wi-SUN FAN adopts IPv6 and supports multi-hop routing using the IPv6 Routing Protocol for Low-power and Lossy Networks (RPL) routing protocol [11]. The maximum number of multi-hop stages exceeds 20

[10]. The multi-hop routing uses an intermediate node as a router to ensure secure connectivity even in an area where direct communication is difficult and eliminates the dead zone.

Since the technical specifications were developed in May 2016, there has been extensive research conducted on Wi-SUN FAN 1.0. Generally, these studies present: a method to increase the rate of construction of a multi-hop network [3], a performance comparison of the average transmission success rate between the MAC layer protocol in Wi-SUN FAN and the TSCH protocol [4], a method to construct a communication path in a multi-hop network that is robust to variation in the communication environment [5], and a method to manage FH to increase the throughput [6]. In February 2019, Wi-SUN Alliance certified interoperable radio devices between manufacturers compliant with Wi-SUN FAN 1.0 [7]. A radio device developed by the author's research group was one of the world's first certified radio devices [7]. Because the Wi-SUN FAN system has not been standardized for a long time, there is no concise document with detailed standard specifications, and there was also no reference data available to evaluate the transmission performance of the Wi-SUN FAN network. The contributions of this study are as follows:

- Many voluminous technical specifications of the Wi-SUN FAN 1.0 are reviewed and concisely summarized. Moreover, the fundamental transmission performance, such as average transmission success rate and average delay time under stable network conditions, is measured using different network topologies in computer simulations as reference data.
- An experimental evaluation environment with actual devices was constructed to validate the transmission characteristics evaluated by computer simulation.
- Using the validated computer simulator, we evaluated the transmission performances of large scale Wi-SUN FAN networks with one border router (BR) and 100 routers arranged in a fixed environment and randomly arranged in a flat square field with 4000 m on a side.

To the best of our knowledge, there are no other studies of validated reference data by both computer simulation and experimental evaluation. The results of this study can be used as reference data to evaluate the actual Wi-SUN network and to design communication systems based on Wi-SUN FAN 1.0.

The remainder of this paper is organized as follows. Sections II and III explain the specification and routing scheme of Wi-SUN FAN 1.0, respectively. Section IV evaluates the transmission success rates and transmission delay times of packets in multiple small-scale Wi-SUN FAN topologies via computer simulations. Section V validates the results of the computer simulation by experimental evaluation involving actual devices. Section VI evaluates the transmission performances of large-scale Wi-SUN FAN networks with one BR and 100 routers and discusses the feasibility of high frequent data transmission in IoT environment. Finally, Section VII concludes this paper.

Layer		Protocols	
Layer 4: Transport		UDP / TCP	IEEE 802.1X
Layer 3: Network		IPv6 / ICMPv6 / RPL / 6LoWPAN	
Layer 2: Data Link	LLC	L2MESH (Option)	
	MAC	IEEE 802.15.4-2015	Security
Layer 1: Physical			

FIGURE 2. Protocol stack standardized as Wi-SUN FAN 1.0.

II. WI-SUN FAN 1.0

A. PROTOCOL STACK

Fig. 2 presents a protocol stack in Wi-SUN FAN 1.0, which is standardized as IEEE 2857-2021 [10]. Wi-SUN FAN defines the physical (PHY), data link, network, and transport layers corresponding to layers 1 through 4 in the OSI reference model. The data link layer is further divided into the upper Logical Link Control (LLC) sublayer and the lower Medium Access Control (MAC) sublayer. Hereafter, the MAC sublayer is referred to as the MAC layer in this study. The network and transport layers provide communications with User Datagram Protocol (UDP) or Transmission Control Protocol (TCP) based on IPv6. Moreover, Wi-SUN FAN supports various security technologies, such as the IEEE 802.1X, IEEE 802.11i, and Extensible Authentication Protocol Transport Layer Security (EAP-TLS), to realize secure communication. A network called the Personal Area Network (PAN) is constructed in Wi-SUN FAN 1.0 by connecting radio devices called "nodes" which directly communicate with each other.

B. PHY LAYER

The PHY layer of Wi-SUN FAN conforms to the IEEE 802 15.4-2015 standard [2], [8]. IEEE 802.15.4-2015 defines three types of modulation schemes for Smart Utility Network (SUN): Frequency Shift Keying (FSK), Orthogonal Frequency Division Multiplexing (OFDM), and Offset Quadrature Phase-Shift Keying (O-QPSK) [2], [8]. In Wi-SUN FAN 1.0, FSK is adopted as a transmission scheme for physical layers with data rates of 50, 100, and 150 kbps [10]. The operating frequency, maximum transmission power, and transmission rate are determined according to the national regulations [2], [10]. Furthermore, the data frame in the physical layer used in Wi-SUN FAN 1.0, which is called the Physical Layer Packet Data Unit (PPDU), stores the MAC layer frame in a payload field called the Physical Layer Convergence Protocol Data Unit (PSDU) [2].

C. MAC LAYER

The MAC layer defines functions related to detecting connectable PAN and participating in PANs, as well as media access control functions for multiple nodes to share and communicate with media, such as frequency, time, etc. The MAC layer of Wi-SUN FAN uses CSMA/CA standardized in IEEE 802 15.4-2015 as the media access control method [8]. Additionally, FH is utilized to avoid the collision of

frames by periodically switching the channels to be used. The CSMA/CA and FH are described in detail below.

1) CSMA/CA

CSMA/CA is used to reduce the packet collision probability by performing clear channel assessment (CCA), which detects the communication of other nodes via channel sensing after waiting for a random length backoff period before sending the packet. The length of the backoff period is determined by multiplying the unit backoff time by a random number ranging from 0 to $2^{BE}-1$, where BE represents a constant called the backoff exponent. A node in the backoff period can receive packets, and the backoff operation is aborted if a packet is received. The backoff operation is resumed after the packet is received, and the node waits for the remaining backoff period. Additionally, if the channel is available, the packet is transmitted without detecting any carrier using the CCA; however, if the carrier is detected and the channel is unavailable, the BE is incremented by 1, up to the maximum backoff exponent. If the number of backoffs is less than or equal to the maximum number of backoffs, the node waits again. The packet is retransmitted if the number of backoffs, NB, exceeds the maximum number of backoffs and if the number of packet retransmission is less than or equal to the maximum number of retransmissions. A binary exponential backoff method is used to increase the range of the backoff period by a factor of two, which reduces the probability of packet collisions in CSMA/CA, where an acknowledge (ACK) frame is received within a certain period after a packet is transmitted.

2) FREQUENCY HOPPING (FH)

The FH scheme is utilized to avoid interference between the links by switching multiple operational frequency channels [6]. Each node performs a receiving operation corresponding to a channel schedule which specifies the order of channels to be used. Because the receiver performs channel hopping, the receiver has no need to know the channel used by the transmitter, but the transmitter needs to know the channel used by the receiver. Wi-SUN FAN employs two transmitting modes in channel scheduling: unicast and broadcast, which use a unicast schedule and a broadcast schedule, respectively. The unicast schedule is generated based on the MAC address of the node, and it differs for each node. The unicast schedules specify the channels to wait for each time interval, which is called the unicast dwell interval (UDI). Conversely, broadcast schedules are generated based on the values unique to PAN, called broadcast schedule identifiers (BSI), which are advertised to all nodes in PAN and are common among all the nodes belonging to PAN. The unicast and broadcast schedules are shared among neighboring nodes and among all nodes in the PAN, respectively, by means of PC frames. If the receiving channel used by a node is unknown at the beginning of the connection, each node conveys the unicast schedule to other nodes by transmitting it on all channels used for FH [6], [10]. Broadcast is accomplished by using
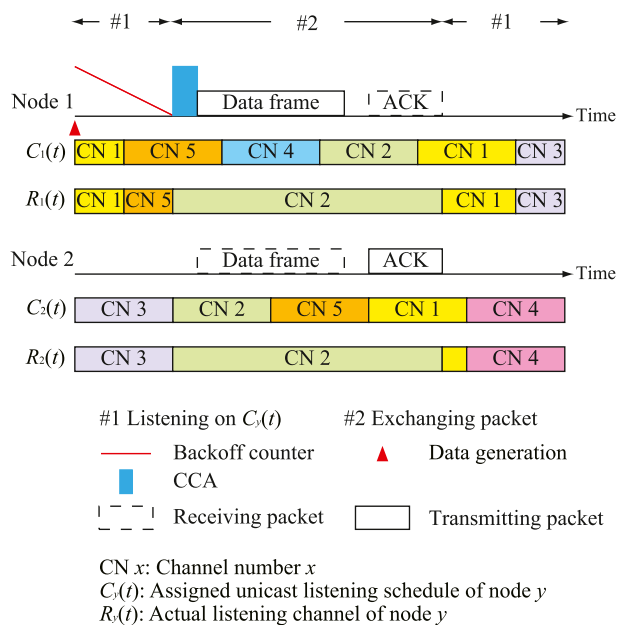
FIGURE 3. Packet transmission in unicast.

FIGURE 4. Operation of a node in Wi-SUN FAN.

a common channel defined by the broadcast schedule for all nodes. Broadcast scheduling defines a time interval, called the Broadcast Dwell Interval (BDI), for each Broadcast Interval (BI) during which a broadcast is to be performed. During the BDI, each node waits for reception on the channel specified in the broadcast schedule in preference to the unicast schedule. Conversely, during the periods other than the BDI, each node awaits reception by the unicast schedule on its own channel. When the packet is transmitted to the node performing FH, the operations in the unicast and broadcast are presented as follows.

a) For unicast: Fig. 3 presents an example of the unicast packet transmission. Following packet generation, the transmitting node performs a backoff operation using CSMA/CA while awaiting reception on the channel based on its channel schedule. Once the backoff operation is completed, based on the shared unicast schedule information, CCA is performed on the channel in which the destination node is awaiting reception. Transmission is performed if the channel is available. However, transmission by unicast is not initiated during the time when the broadcast channel is valid in the broadcast schedule, and it waits until the destination node starts receiving information based on the unicast schedule. Subsequently, the node which initiated the communication continues communicating on the same channel without switching until the packet is transmitted and the reception confirmation is generated by the ACK frame. The node awaits reception on a channel based on its unicast schedule once again when the communication is completed.

b) For broadcast: A broadcast packet is transmitted only for the BDI period, during which a broadcast channel is allocated for each BI. The transmitting node transmits on the channel
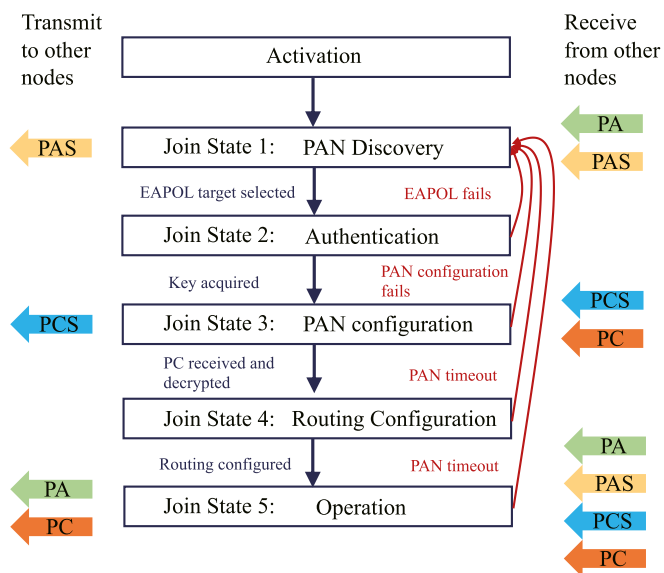
defined by the broadcast schedule. The channel function determines the unicast and broadcast schedules. Wi-SUN FAN employs the directed hash channel function (DH1CF) [10] as a channel function. In the DH1CF, the channel schedule is obtained by using the current time, schedule identifier, and the number of channels to be used. For a unicast and broadcast schedule, the MAC address of the node and PAN-specified BSI are utilized as the schedule identifier, respectively.

D. NETWORK LAYER

Wi-SUN FAN uses IPv6 as the network-layer protocol. In addition to reporting the error information during packet processing, Internet Control Message Protocol for IPv6 (ICMPv6) is used to provide various functions, such as address resolution, multicast, and duplicate IPv6 address detection. Wi-SUN FAN supports multi-hop communication using IPv6 and can transmit packets in both directions based on the constructed path. A routing protocol called RPL is adopted for low-power and lossy networks (LLNs) in the network layer [10], [11], and each node autonomously selects a parent node to construct; it then changes and maintains the necessary paths for multi-hop communication corresponding to changes in the propagation environment. Section III presents a detailed description of RPL.

E. BASIC OPERATION OF INTER-NODE COMMUNICATION

In Wi-SUN FAN 1.0, a PAN is developed by connecting nodes that directly communicate with each other. This section describes the various control frames used for detecting PANs and participating in a PAN. Fig. 4 depicts the operation performed by a node in each connection state, and the underlying process is described below.

1) PAN CONTROL FRAME

In Wi-SUN FAN, each node primarily uses the following four control frames to detect and participate in PANs.

- *PAN advertisement (PA) frames:* A frame that enables the nodes joined to a PAN to inform the nodes that do not participate in the PAN, of the minimum information required for PAN discovery and selection.
- *PAN advertisement solicit (PAS) frames:* A frame that enables the nodes that have not joined a PAN to request a node that has joined the PAN, to transmit the PA frames more frequently.
- *PAN configuration (PC) frame:* A frame that enables a node participating in the PAN to present the information of the group key, channel schedule, current time, etc.
- *PAN configuration solicit (PCS) frame:* A frame that can be used to request the nodes that have not been participating in the PAN to transmit the PC frames more frequently to the nodes that have already participated in the network.

2) CONNECTION STATUS

Fig. 4 illustrates each connection status and operation until a node completes the network layer routing and transmits the user data. The operation is explained in detail below.

a) Join State 1. PAN selection: This is the initial state of the node, and in this state, a node does not yet contain the information on the neighboring nodes or the PAN. The node transmits PAS frames at intervals controlled by the trickle timer [12] and requests the node belonging to the PAN to transmit the PA frames. When a PA frame is received at the node, the information on the neighboring node is added to the Extensive Authentication Protocol over LAN (EAPoL) candidate list. The EAPoL candidates list is used to determine the PAN with which the node attempts to connect. Once a node determines a connecting node from the EAPoL list within the selected PAN, the connecting status proceeds to Join State 2.

b) Join State 2. Certification: In this state, the node executes the IEEE 802.1X/802.11i security flow and performs authentication and key acquisition. If authentication and key acquisition are successfully completed, the node is set to the same PAN ID as the EAPoL destination, and the connecting status proceeds to Join State 3. If authentication and key acquisition fail, the connecting status returns to Join State 1.

c) Join State 3. PAN Settings: The node sends the PCS frames at intervals controlled by the trickle timer and requests PC frames to the nodes belonging to the PAN. If a PC frame can be received, the connection status proceeds to Join State 4. However, if a PC frame cannot be received even after a certain number of PCS frames have been transmitted, the connecting status returns to Join State 1. In this case, the trickle timer is standardized by IETF for controlling the transmission interval
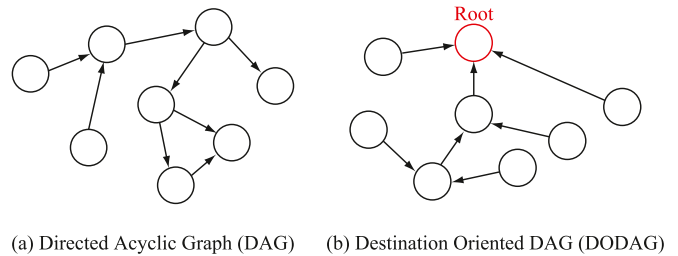

(a) Directed Acyclic Graph (DAG) (b) Destination Oriented DAG (DODAG)

FIGURE 5. Examples of DAG and DODAG.

of the control frame of the network [3], [12]; it is explained in more detail in Section III. B.

d) Join State 4. Route construction: In state 4, the node has completed participating in the PAN, and network layer routing has been performed. If the node can establish connectivity with the BRs within a certain period, the connecting status proceeds to Join State 5, else the node returns to Join State 1 if connectivity cannot be established within a certain period.

e) Join State 5. Connected: In this stage, the network layer routing is complete. The PA and PC frames continue to be transmitted at intervals controlled by the trickle timer. If the node is disconnected with BR for a certain period, the status returns to Join State 1. Moreover, the BRs consistently maintain Join State 5.

III. ROUTING SCHEME BY RPL

Wi-SUN FAN adopts RPL [5], [10], [11] as a routing protocol in the network layer to support multi-hop communication using IPv6. This section describes the network model in RPL and the various control messages. Additionally, the routing metrics and routing construction schemes defined in Wi-SUN FAN 1.0 are also described.

A. NETWORK MODEL

RPL constructs a network of topologies based on a directed acyclic graph (DAG); however, the Destination Oriented DAG (DODAG) is directed without a cyclic graph. The DODAG comprises a root node without any outgoing edges. Fig. 5 presents both the DAG and DODAG. In the RPL, the route from any node in the DODAG to the root node is defined as the upstream route, and the route from the root node to any other node in the DODAG is defined as the downstream route. Two principal methods are used to determine the downstream routes: the storing mode and the non-storing mode. In the storing mode, each node retains a routing table for a lower-rank DODAG, data routing is forwarded based on the routing table, and the downstream route is established. In the non-storing mode, nodes other than the root node do not retain the routing table, and the route node determines the downstream routes and presents this information to the other nodes. Wi-SUN FAN utilizes RPL with the non-storing mode. Each node which configures a multi-hop PAN in Wi-SUN

FAN is categorized into the following three types based on its function, as illustrated in Fig. 1(b).

- *Border router (BR):* The root node of a DODAG, which is located per PAN, is used to perform authentication, key management, and access the wide area network (WAN). Moreover, BR has a routing table for the entire DODAG to determine the downstream routes.
- *Router:* It can have a parent node and child nodes, and it generates and forwards packets.
- *Leaf:* It has minimal functionality, such as packet-generation, transmission, and reception. Since it does not have the packet forwarding function, it becomes a terminal node without a child node.

RPL assigns an ID called RPL instance-ID to each network, where a set of DODAGs with the same RPL instance-ID is called the RPL instance.

B. TRICKLE TIMER

The trickle timer [3], [12] controls the transmission interval of the control frames of the network. It reduces the traffic generated by the control frames by exponentially increasing the transmission interval when the network is stable. Conversely, if the network is unstable, the trickle timer reduces the transmission interval to stabilize the network by frequently transmitting control frames.

C. CONTROL MESSAGE

In RPL, the following control messages are used for routing.

- *DODAG Information Object (DIO):* Transmitted to obtain the information required to select the parent and maintain DODAG. The nodes participating in the RPL network broadcast DIO at the timing determined by trickle timer [3], [12]. The DIO contains information on the rank of the sender, and the node receiving the DIO selects the parents based on this information. The exception is that Leaf does not send a DIO because it cannot have children.
- *DODAG Information Solicitation (DIS):* Transmitted from the nodes that do not participate in RPL network to request the DIO for nodes in the RPL network. These nodes broadcast the DIS at regular intervals.
- *Destination Advertisement Object (DAO):* Transmitted to construct and maintain a downstream route from the BR to the nodes that participate in the RPL network. In Wi-SUN FAN, the non-storing mode RPL is used, and the nodes participating in the network present their parent information to the BR by using DAO. The BR performs source routing of the downstream routes based on the parent information of each node. The DAO is unicast at regular intervals from each node to the BR.
- *DAO-ACK:* Is used to verify whether the DAOs have propagated to the BR. If the BR does not return the DAO-ACK within a certain period, the node which transmitted the DAO performs retransmissions.

D. ROUTING METRIC

RPL in Wi-SUN FAN utilizes the exponentially weighted moving average (EWMA) of the received signal level (RSL) and the expected transmission count (ETX) as link metrics between the nodes. The EWMA is an exponentially weighted moving average for a given series, $X(t)$, and is given by the following equation:

$$X_{\text{EWMA}}(t) = S_{\text{M}}X(t) + (1 - S_{\text{M}})X_{\text{EWMA}}(t-1), \quad (1)$$

where S_{M} denotes a smoothing factor that satisfies $0 < S_{\text{M}} < 1$, and $X_{\text{EWMA}}(0) = X(0)$. In Wi-SUN FAN, $S_{\text{M}} = 1/8$ [10]. RSL and ETX are defined as follows:

- *RSL:* A metric based on the received power, with a bias of 174 added to it ranges from −174 to + 80 dBm; this metric is expressed as a value ranging from 0 to 254. RSLs are defined from the neighboring nodes to the self-node, and from the self-node to the neighboring nodes. The RSL from a neighboring node to the self-node is obtained based on the power received from the neighboring node. The RSL from the self-node to the neighboring node is obtained based on the received power of the transmitted packet at the neighboring node and is transmitted from the neighboring node to the self-node via an ACK frame. The received power is based on energy detection of PHY layer.
- *ETX:* A metric based on the transmission success rate of a frame, defined in Wi-SUN FAN as follows:

$$\begin{cases} \lambda = 128 \cdot T/S = 128/\varpi & (T/S < 8) \\ \lambda = 1024, & (T/S \geq 8) \end{cases} \quad (2)$$

where T denotes the number of transmission attempts of the frame, S denotes the number of reception times for ACK frame, and ϖ symbolizes the transmission success rate. The EWMAs of RSL and ETX are calculated for all the packets acknowledged by the ACK frame. The ETX is calculated and the EWMA of ETX is updated when four or more transmissions have been performed since the last ETX was calculated and more than one minute has elapsed. Moreover, the ETX is calculated for a single transmission attempt immediately when the node is initiated.

In RPL, the Objective Function (OF) provides each node a means to select and optimize the routes. In Wi-SUN FAN, minimum rank with hysteresis objective function (MRHOF) is used as an OF [5], [13]. In the RPL using MRHOF, the path-cost and rank are adopted as indices to configure the route. These terms are defined as follows:

- *Path cost:* An indicator to evaluate the path to the BR. The MRHOF preferentially selects a path with a lower path cost. In Wi-SUN FAN, the path cost can be determined by the sum of the rank of the parent and the EWMA of ETX to the parent. The path cost when a node, N, selects the candidate parent, κ, is given as follows:

$$\vartheta_N(\kappa) = \min\{\lambda_{\text{EWMA}}(N, \kappa) + \varrho(\kappa), 32768\} \quad (3)$$

where $\lambda_{\text{EWMA}}(N, \kappa)$ represents the EWMA of ETX for parent node, κ, at node, N. $\varrho(\kappa)$ represents the rank of the parent node, κ, which is notified by DIO.

- *Rank:* An indicator of the relative position to the BR in the network. The rank increases as a node moves away from the BR. In Wi-SUN FAN, the rank of node, N, with the parent of node, κ, is given as follows:

$$\begin{cases} \varrho(N) = \hat{A}, & (N : \text{BR}) \\ \varrho(N) = \max[\min\{\varrho(\kappa) + \hat{A}, & (N : \text{Other}) \\ 65535\}, \ \vartheta_N(\kappa)], \end{cases} \quad (4)$$

where $\hat{A}$ represents the smallest rank, and $\hat{A} = 128$ in Wi-SUN FAN.

E. ROUTING PROCEDURES
In RPL using MRHOF, routing with hysteresis properties is performed to preferentially select the paths with low path cost while preventing frequent changes in the network caused by minor changes in the metrics. The route construction procedure for the upstream route is described below.

1) *Creating a candidate parent set:* Each node creates a list of neighboring nodes whose EWMA of RSL exceeds a predetermined threshold. This list of neighboring nodes is called a candidate parent set. Additions and exclusions to the candidate parent set are performed based on the conditional equation with the following hysteresis characteristics:

- A node, N, adds a neighboring node, ξ, to the candidate parent set when both EWMAs of the bidirectional (i.e., downstream and upstream) RSLs for the neighboring node, ξ, satisfy the following equation:

$$\iota(N, \xi) > \hat{X} + \hat{Y} + \hat{Z}, \quad (5)$$

where $\iota(N, \xi)$ represents the EWMA of RSL, $\hat{X}$ denotes the vendor-dependent minimum receiver sensitivity level, $\hat{Y}$ denotes the constant which defines the threshold for adding the candidate parent set, and $\hat{Z}$ denotes the hysteresis constant. In Wi-SUN FAN, $\hat{Y} = 10$ and $\hat{Z} = 3$.

- The node, N, excludes its neighboring node, ξ, from the candidate parent set when both EWMAs of the bidirectional RSLs for the neighboring node, ξ, satisfy the following equation:

$$\iota(N, \xi) < \hat{X} + \hat{Y} - \hat{Z}. \quad (6)$$

2) *Calculating the path cost:* The node derives the path cost $\vartheta_N(\kappa)$ for the candidate parents in the candidate parent set by using the rank $\varrho(\kappa)$ notified by the DIO.

3) *Parent decision:* Selects the candidate parent for which the path cost $\vartheta_N(\kappa)$ is the lowest in the candidate parent set. Since the MRHOF has a hysteresis function, the node maintains a connection with the current parent if the difference between the path costs for the current parent and the new parent is less than the threshold $\hat{T}$. In MRHOF, the parent selection is performed in the following cases:

- The path cost for parent and candidate parents is updated.
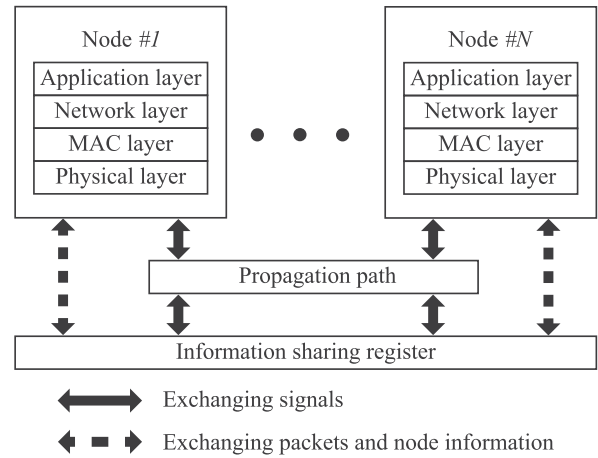- A new candidate parent is added.

FIGURE 6. Configuration of the computer simulation.

A downstream route is established after establishing an upstream route. The route development procedure for the downstream route is outlined below.

- The node transmits a neighbor solicitation (NS) and registers its own IPv6 address with its parent, allowing the BR to return the DAO-ACK.
- The node unicasts a DAO containing its IPv6 address along with its parent' to the BR.
- The BR registers information in the DAO with the routing table. Moreover, it determines the downstream route and transmits the DAO-ACK back to the node.
- The routing of the downstream route is completed when the node receives the DAO-ACK. The DAO is retransmitted if DAO-ACK cannot be received within a certain period.

IV. PERFORMANCE ANALYSIS IN MULTIPLE SMALL-SCALE WI-SUN FAN TOPOLOGIES BY COMPUTER SIMULATION
This section evaluates the fundamental transmission characteristics in multiple small-scale Wi-SUN FAN networks using RPL. In this study, a computer simulator was developed for Wi-SUN FAN to evaluate different transmission characteristics, such as the transmission success rate and delay time for packet generation rate.

A. OVERVIEW OF COMPUTER SIMULATOR
Fig. 6 presents the configuration of the computer simulator used in this study. Originally, the computer simulator was developed for Wi-SUN FAN using C# based on [14] and can flexibly set various parameters related to the system model, propagation model, and communication functions. The computer simulation environment primarily comprises nodes, propagation paths, and information sharing registers. A node is a component which corresponds to a generated Wi-SUN FAN node depending on the number of nodes to be simulated. Each node is independently operated and cannot directly refer to the information of the other nodes. A node

provides the physical, MAC, network, and application layer functions, which are defined below.

- *Application layer:* Generates UDP packets based on the packet generation rate. The generated packets are forwarded to the network layer, and the received UDP packets are recorded.
- *Network layer:* Performs routing using RPL. The packets transmitted from the application layer are transmitted to the destination based on the route.
- *MAC layer:* Transmits packets using the CSMA/CA. FH is performed by generating various channel schedules are generated. Additionally, the ETX and RSL used as link metrics in the RPL are calculated and transmitted to the network layer. Retransmissions are performed at the MAC layer, and CSMA/CA is used. If the buffer is full due to retransmissions and a new packet arrives, the most recent packet is dropped.
- *Physical layer:* Receives a transmission request from the MAC layer and transmits the signal. In this layer, the delay time associated with the reception switching of the radio is simulated. Additionally, the propagation path is monitored, and the start of the packet reception and collision are determined. The determination of the collision is made as packet loss if CINR (Carrier to interference plus noise power ratio) of the desired packet is less than or equal to a predetermined threshold, and as packet transmission success if the CINR is greater than the threshold.

The propagation path defines a radio wave propagation model that attenuates signals based on the path model set beforehand, which corresponds to the positions of the nodes. The information-sharing register registers the information that is to be shared between the nodes. If a node requires information from another node, it consults the information sharing register. Examples of the information registered in the information sharing register include information on the transmitted signals and packets, node location, and channel schedules.

B. EVALUATION SYSTEM

A small-scale Wi-SUN FAN system is evaluated with star and tree topologies using a total of 20 nodes, one BR, and 19 routers, to compare the characteristics with the actual system. The evaluation assumed an upstream route where 19 routers transmit their information to the BR. Fig. 7 presents all the network topologies evaluated in this study. A propagation model which does not result in power loss between the transmitting and receiving nodes is used in the computer simulation. To avoid disrupting the topology, MAC filtering is performed to discard packets when the source MAC address is specified in the MAC layer. The MAC filters can be set individually for each node. In a star topology network, the BR is configured to receive packets from all nodes. Additionally, the router is set to be able to only receive packets from the BR by MAC filtering.

In a tree topology network, each node is configured to only communicate with a particular node through MAC filters, and
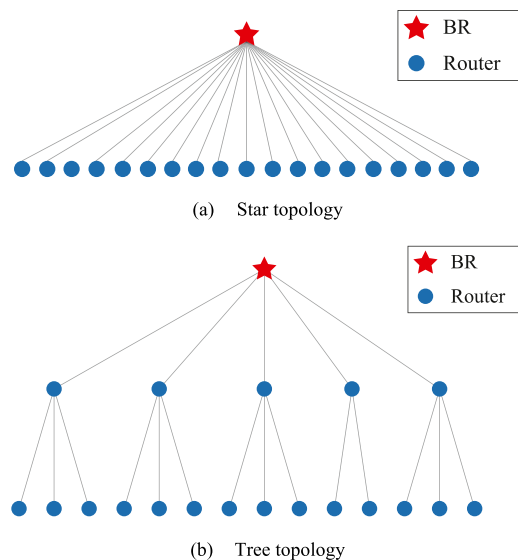

FIGURE 7. Topology used in this study.

a particular path is constructed. In total, 19 routers are divided into two groups based on the routing of the packets transmitted from the BR. A group where the number of transferring packets from a node to BR is one is set as Group 1, and five routers were allocated. Subsequently, a group where the number of transferring packets from a node to BR is two is set as Group 2, and 14 routers were allocated. The BR can only receive packets from routers in Group 1 by MAC filtering. A router in Group 1 can receive packets only from the BR, and the nodes in Group 2 which are the child nodes of the router. A router in Group 2 can only receive packets from the node in Group 1 which is the parent node of the router.

In computer simulations, the transmission is evaluated based on the assumption that the development of PAN is completed. Routing by RPL is initiated, and each node starts to generate data packets independently. UDP is used to generate data packets after a certain period; the data packets are generated at regular intervals based on the specified frequency. In this study, such a data packet is simply referred to as a "packet". The packets are forwarded to the BR using unicast according to the constructed upstream route. To evaluate the steady-state characteristics of the network, the measurement was performed after the 50th packet was generated at the node. The generation of the packet continues until the simulation is completed, and the simulation continues until there are no packets left to be measured from the packet buffer of all the nodes. Moreover, a node that fails to communicate with the BR and moves to Join State 4 or less does not send a packet, and in such a case, the packet generated at the node is discarded. Tables 1–3 present the parameters used in this study. The number of channels was used for 1 and 14 to determine the effect of FH.

C. METRICS FOR EVALUATION

In this study, the transmission success rate and delay time are used as indices to evaluate the transmission efficiency in the

TABLE 1. Parameters Related to the Node

Parameter	Value
Number of routers	19 (Section IV), 100 (Section VI)
Transmit power	13 dBm (Section IV)
Number of target data packets per router	100
Data packet length	340 bytes
Packet generation rate	From 1.00×10^{-2} to 1.00 s^{-1}
Data rate	150 kbps
RSSI threshold	−104 dBm
CCA threshold	−84 dBm
Packet buffer size	15

TABLE 2. Parameters Related to the MAC Layer

Parameter	Value
UDI	250 ms
BI	1 s
BDI	0.1 s
Number of channels	14, 1
Minimum backoff exponent	4
Maximum number of backoff	4
Maximum number of backoff	5
Maximum number of retransmissions	4
Unit backoff time	5.3 ms
ACK frame length	72 bytes

TABLE 3. Parameters Related to the RPL

Parameter	Value
DIS sending interval	30 s
Minimum DIO trickle timer I_{min}	1.024 s
Maximum DIO trickle timer I_{max}	7
DAO sending interval	600 s
Maximum number of DAO retransmission	5
DAO retransmission interval	10 s
Neighbor solicitation sending interval	600 s
Size of candidate parent set	4

network. The transmission success rate is defined as the ratio of the number of packets successfully received in the BR to the number of packets generated in the node. The delay time includes the average time since a packet was generated at the node until it is received at the BR. However, the packets that have not reached the BR are excluded from the delay time calculation. Additionally, the number of child nodes and the number of contention nodes at each node are used as indices to evaluate the constructed routes. The number of child nodes is defined as the number of nodes connected to each node, and the number of contention nodes is defined as the sum of the number of nodes passing through one or more common routers in the path to the BR.

D. RESULTS AND DISCUSSION

First, the transmission characteristics in a star topology network are explained. Table 4 shows the relationship between the packet generation rate and the average transmission success rate in the BR when the number of target data packets

TABLE 4. Average Transmission Success Rate in the BR When the Number of Target Data Packets Observed Per Router is Varied

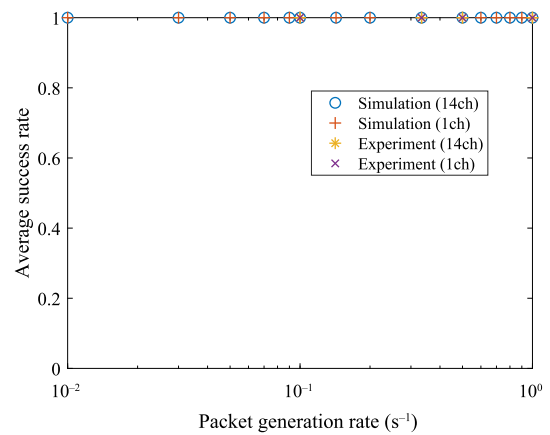| Num. of target packets per router	Star topology, 1 BR, 19 routers, 1 channel			Star topology, 1 BR, 19 routers, 14 channels		
	Packet generation rate (s^{-1})			Packet generation rate (s^{-1})		
	1	10^{-1}	10^{-2}	1	10^{-1}	10^{-2}
100	1.0			1.0		
1000	1.00			1.00		
10000	1.000			0.9997		1.000

FIGURE 8. Average transmission success rate (star topology).

observed per router is varied. Since the data packets are generated at regular intervals based on the specified frequency and are not generated randomly, the average transmission success rate does not change significantly when the number of target data packets per router is varied. In this study, the number of target data packets per router is set to 100 to reduce simulation time.

Fig. 8 presents the average success rate characteristics of all the nodes corresponding to the packet generation rate, where the packet generation rate is defined as the reciprocal of the number of packets generated per second. In the computer simulation, the average success rate in the range of packet generation rate was maintained at 1, regardless of the presence or absence of FH. Fig. 9 presents the average delay time characteristics of all the nodes for the specified packet generation rate. The average delay time is not lower than approximately 65 ms even in a relatively low domain of packet generation rate of $1.00 \times 10^{-1} \text{ s}^{-1}$ or less. This can be attributed to the delay due to the backoff time and the transmitting time of the packets in the CSMA/CA.

Table 5 presents a breakdown of the packet transmission processing time when there are no backoff retries or packet retransmissions. The average packet transmission processing time is 65.801 ms, which is roughly consistent with the simulation evaluation results when packets are generated infrequently. However, the average delay time increases when the packet generation rate is $5.00 \times 10^{-1} \text{ s}^{-1}$ or more. The average delay time is approximately 0.16 s when one channel
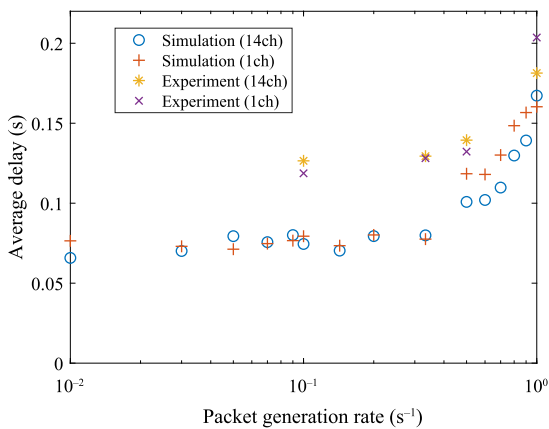
FIGURE 9. Average delay time to successfully transmit packet (star topology).

TABLE 5. Breakdown of the Packet Transmission Processing Time

Items	Minimum	Average	Maximum
Backoff	5.3 ms	42.4 ms	79.5 ms
CCA		0. 128 ms	
Transmitter preparation		0.2 ms	
Data packet transmission		18.133 ms	
Tack		1.1 ms	
ACK transmission		3.84 ms	
Total	28.701 ms	65.801 ms	102.901 ms
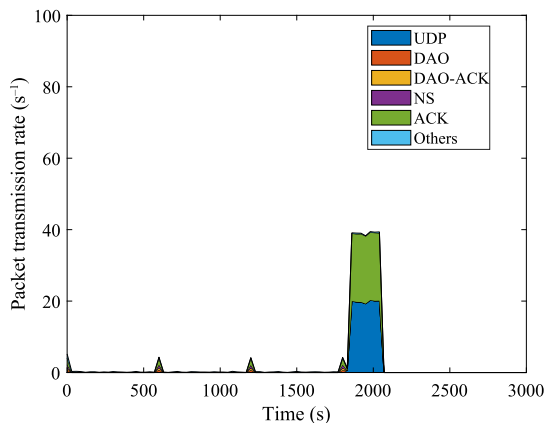
FIGURE 10. Breakdown of the number of packets transmitted per unit time when the packet generation rate is 1.00 s^{-1} and the number of channels used is one (Star topology, simulation).

is used and the packet generation rate is 1.00 s^{-1}. This is caused by the backoff retries and packet retransmissions as the number of transmitted packets increases.

Fig. 10 presents a breakdown of the number of packets transmitted per unit time when one channel is used and the packet generation rate is 1.00 s^{-1}. In this study, the number of packets transmitted per unit time is referred to as the packet transmission rate. In Fig. 10, the horizontal axis represents the elapsed time from the start of the simulation, and the vertical axis represents the total packet transmission rates of

TABLE 6. Breakdown of the Number of Total Packets Transmitted in the Period When UDP Packets are Transmitted (Star Topology, Simulation, 1 Channel)

Packet generation rate (s^{-1})	Time (s)	Packet count					
		UDP	DAO	DAO ACK	NS	ACK	Other
1.00×10^{-2}	26232.7	4982	820	820	1023	7434	4006
1.00×10^{-1}	2623.9	4985	79	77	94	5212	402
3.33×10^{-1}	787.7	5007	19	20	19	5048	120
5.00×10^{-1}	420.0	4075	0	0	0	3990	65
1.00	209.7	4169	0	0	0	3984	40

TABLE 7. Average Transmission Success Rate in the BR When the Number of Target Data Packets Observed Per Router is Varied

Num. of target packets per node	Tree topology, 1 BR, 19 routers, 1 channel			Tree topology, 1 BR, 19 routers, 14 channel		
	Packet generation rate (s^{-1})			Packet generation rate (s^{-1})		
	1	10^{-1}	10^{-2}	1	10^{-1}	10^{-2}
100	0.59	1.0		1.0		
1000	0.596	1.00		1. 00		
10000	0.5964	1.000		0.9995	1.000	

all the nodes by stacking various types of rates. In this figure, the packet transmission rate is measured every 30 seconds. Table 6 presents a breakdown of the number of packets transmitted in the period when UDP packets are transmitted. The total transmission rate of the UDP packet of all the nodes is approximately 19.9 s^{-1} (4169 packets/209.7 s) after 1860 seconds of initiating the data packet generation. Conversely, the total packet generation rate of all the nodes is 19 s^{-1}, which indicates that some packets have been retransmitted. In the star topology network, the transmission characteristics, such as the average transmission success rate and average delay time, do not vary significantly corresponding to the number of channels used. In such a case, it is difficult to present interference avoidance by FH even if multiple channels are available.

Second, the transmission characteristics in a tree topology network are discussed. Table 7 shows the relationship between the packet generation rate and the average transmission success rate in the BR when the number of target data packets observed per router is varied. For the same reasons as in star topology, the average transmission success rate does not change significantly when the number of target data packets per router is varied. In this study, the number of target data packets per router continues to be set to 100 to reduce simulation time. Fig. 11 presents the average transmission success rate characteristics of all the nodes corresponding to the packet generation rate. The average transmission success rate was maintained at approximately 1 across the entire range of the evaluated packet generation rate when the FH with 14 channels was used. Conversely, the average transmission success rate drops in the region where the packet generation rate is greater than 7.00×10^{-1} s^{-1}, and when the packet generation rate is 1.00 s^{-1}, the average transmission success rate is approximately 0.59, in the case when the number of channels
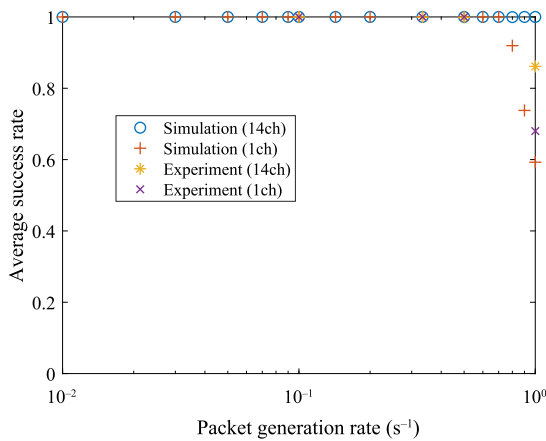
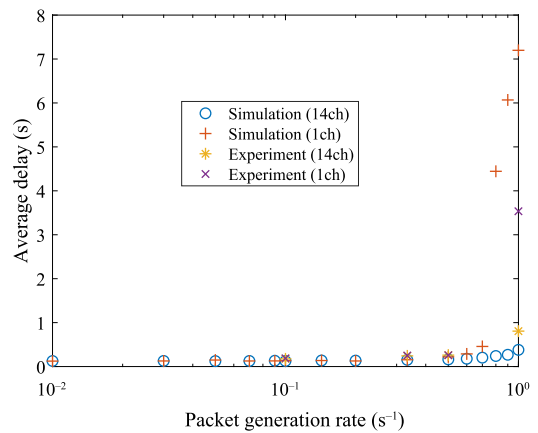FIGURE 11. Average transmission success rate (tree topology).

FIGURE 12. Average delay time to successfully transmit packet (tree topology).

TABLE 8. Average Number of Packets in Buffer of Each Router

Node index	Packet count (14 channel)	Packet count (1 channel)
Router 1	0.6	13.9
Router 2	0.8	13.6
Router 3	0.5	14.0
Router 4	0.4	14.5
Router 5	0.2	13.5

TABLE 9. Breakdown of the Number of Total Packets Transmitted in the Period When UDP Packets are Transmitted (Tree Topology, Simulation,14 Channels)

Packet generation rate (s⁻¹)	Time (s)	Packet count					
		UDP	DAO	DAO ACK	NS	ACK	Other
1.00×10^{-2}	26223.1	8689	1465	1466	1478	12931	3999
1.00×10^{-1}	2622.8	8735	89	140	148	9064	400
3.33×10^{-1}	630.0	7110	19	38	45	7087	91
5.00×10^{-1}	420.0	7300	0	0	10	7021	62
1.00	262.8	10210	0	0	14	8909	38

used is 1. This can be attributed to the packet dropping due to buffer overflow at each node. Table 8 presents the average number of packets in buffers for five routers whose parent node is the BR when the packet generation rate is 1.00 s⁻¹. Here, the number of packets in the buffer was measured and averaged every 5 seconds from the start of packet transmission. The average number of packets in the buffer is one or less, and packets are transmitted without delay at each node when the number of channels to be used is 14. Meanwhile, when the number of channels to be used is one, the average number of packets in the buffer is 13 or more. Therefore, it is considered that the number of packets to be transmitted exceeds the actual number of packets to be transmitted, resulting in packet discarding due to buffer overflow. Besides, if the number of channels to be used is one, then simultaneous transmission by different nodes cannot be performed, and the number of packets transmitted is suppressed.

The average delay time characteristics of all nodes for packet generation rate are illustrated in Fig. 12. The average delay time is small when the packet generation rate is less than or equal to 1.00×10^{-1} s⁻¹. The delay time is 126 ms when the packet generation rate is 1.00×10^{-2} s⁻¹ and the number of FH channels is 14. In the tree topology network evaluated in this study, there are five routers that perform packet transfer once and 14 routers that perform packet transfer twice, and the average number of transfers is approximately 1.74 times. Therefore, when packet transmission is performed by the average packet transmission processing time presented in

Table 5 at all the nodes, the average delay time is approximately 114 ms. This value is considered as a region where packets generate less frequently, and the delay time asymptotically approaches the same value. The average delay time of all nodes increases with an increase in the packet generation rate. The average delay is approximately 0.38 s if the packet generation rate is 1.00 s⁻¹ and the FH with 14 channels is used. This increase in the average delay time is attributed to the backoff retries or packet retransmissions.

Fig. 13(a) presents a breakdown of the total packet transmission rate for all the nodes when the packet generation rate is 1.00 s⁻¹ and the FH with 14 channels is used. Table 9 presents a breakdown of the number of packets transmitted in the period when UDP packets are transmitted. It is evident that the total of the UDP packet transmission rate at all nodes is approximately 38.9 s⁻¹ (10210 packets/262.8 s) from the time period of 1860 s when the generation of the data packet was initiated until the measurement ends and the generation of UDP packet ends. Conversely, it can be observed that the ACK frame transmission rate by the CSMA/CA in the same time interval is approximately 33.9 s⁻¹. Since the UDP packet transmission rate is higher than the ACK frame transmission rate, a collision occurs in the UDP packet, and packet retransmission is assumed to occur. An increase in the delay time can be caused by a delay produced by a backoff retry or packet retransmission, as explained earlier, a delay due to a wait time
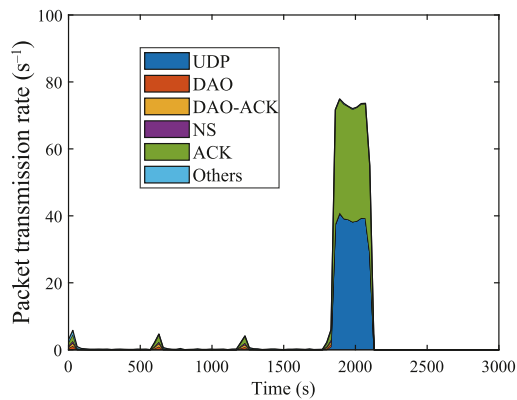
(a) Number of packets sent per unit time (14 channels)
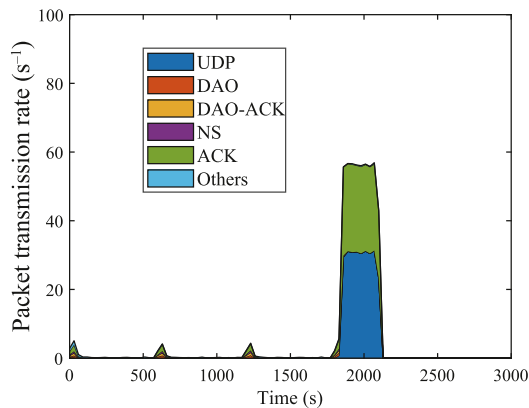
(b) Number of packets sent per unit time (1 channel)

FIGURE 13. Breakdown of the number of packets transmitted per unit time when packet generation rate is 1.00 s^{-1} and the number of channels used is 14 (tree topology, simulation).

TABLE 10 Breakdown of the Number of Total Packets Transmitted in the Period When UDP Packets are Transmitted (Tree Topology, Simulation, 1 Channel)

Packet generation rate (s^{-1})	Time (s)	Packet count					
		UDP	DAO	DAO ACK	NS	ACK	Other
1.00×10^{-2}	26229.8	8655	1431	1428	1472	12931	4003
1.00×10^{-1}	2623.0	8655	136	134	145	9061	400
3.33×10^{-1}	786.9	8705	35	34	46	8763	119
5.00×10^{-1}	420.1	7256	0	0	12	6941	63
1.00	262.8	8069	0	0	12	6667	34

in the packet buffer, or a packet transmission being suppressed owing to a limited number of channels.

Fig. 13(b) presents a breakdown of the total packet transmission rate for all the nodes when the packet generation rate is 1.00 s^{-1} and the number of channels used is one. Table 10 presents a breakdown of the number of packets transmitted in the period when the UDP packets are transmitted. It can be observed that the total of the UDP packet transmission rate at all the nodes is approximately 30.7 s^{-1} from the generation of the data packet to the end of the measurement, and that the number of packet transmissions is suppressed compared
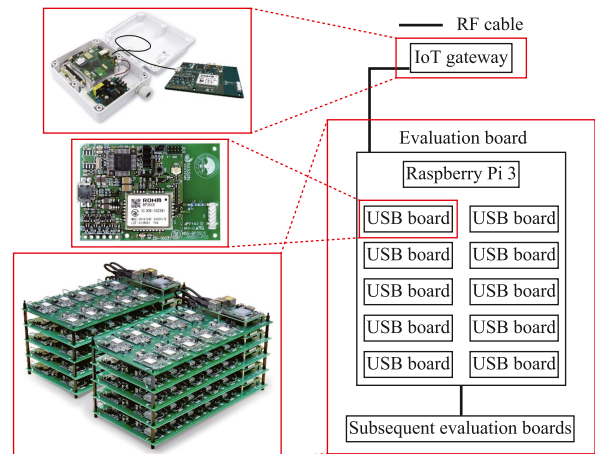

FIGURE 14. Configuration of the Wi-SUN FAN used in the experimental environment.

to the case where the FH with 14 channels is used. There are conflicts in the UDP packets and packet retransmission because the ACK frame transmission rate in the same interval is approximately 25.4 s^{-1}, which is smaller than the UDP packet transmission rate, and the average delay time increases significantly to 7.20 s. It can be observed from the above evaluation that in a tree topology network, the interference between nodes can be avoided by using an FH with multiple channels, and transmission characteristics, such as average transmission success rate and average delay time, are significantly improved.

V. PERFORMANCE VALIDATION OF COMPUTER SIMULATION RESULTS BY EXPERIMENTAL EVALUATION

In this section, the same configuration as the Wi-SUN FAN network evaluated by computer simulation is constructed using actual radio devices, and the results of computer simulation are validated by experimental evaluation.

A. EVALUATION ENVIRONMENT

Fig. 14 depicts the configuration of Wi-SUN FAN used in the experimental environment. Here, the Wi-SUN FAN mounted on USB board was used as a router to configure the Wi-SUN FAN networking. The USB board consists of a Wi-SUN FAN module BP35C5 by ROHM Co., Ltd., chip antenna, and U.FL-type connector for an external antenna, and it can be operated as a Wi-SUN FAN node or used for capturing packets in the module firmware to operate Wi-SUN FAN 1.0 developed in the author's laboratory and certified by the Wi-SUN alliance. A control command can be executed via a micro USB terminal on the board for various operations, such as achieving flexible control of the PHY and MAC parameters, updating firmware, log acquisition, etc. An evaluation board equipped with a Raspberry Pi 3 Model B connected to 10 USB boards operates as a single group. Moreover, the USB boards on the evaluation board can be connected to each other through a U.FL-type connector. Additional USB boards can

be connected to each other by connecting multiple evaluation boards with coaxial cables. In this experimental evaluation, the IoT gateway, NSS-OTDR-GW-V0002 by Nisshin Systems, was used as the BR. The IoT gateway is equipped with a BP35C5 and can perform the functions of the BR, achieve flexible control, change PHY and MAC parameters, perform log acquisition, and other functions. Additionally, the IoT gateway can handle neighboring node information of up to 1024 units, and a large-scale FAN network can be constructed and evaluated. The evaluation boards and IoT Gateway are connected to a control Windows PC, which executes various commands based on the measurement scenarios, collects logs, and synchronizes the time between the USB boards.

B. SPECIFICATIONS OF EXPERIMENTAL EVALUATION

The transmission performance of 20 nodes were evaluated with a BR and 19 routers. The nodes were connected via an evaluation board, and two evaluation boards were connected to the IoT gateways configured as a BR using coaxial cables. Two types of networks were evaluated: star topology and tree topology. For each network, the MAC filters, similar to those shown in Section IV, were set and the nodes that can be connected to each node were restricted.

When starting the measurement, the BR was started after all the routers were started. The DAO transmit interval in the router was set at 60 s to increase the frequency of updating the routing table in the BR during the construction phase of the network. Once all the routers complete routing through RPL and verify that they are registered in the routing table of the BR, they start generating the packets using UDP. The packet generation rates are 1.00×10^{-1} s^{-1}, 3.33×10^{-1} s^{-1}, 5.00×10^{-1} s^{-1}, and 1.00 s^{-1}. The packets are generated at regular intervals based on the specified packet generation rate. During the measurement, packets were captured at each node. The transmitting power of each node was set to zero dBm. The other parameters are identical to those presented in Section IV.

C. METRICS FOR EVALUATION

The metrics for the experimental evaluation were essentially identical those defined in Section IV. Moreover, the received power from the routers in the BR and the network-configuration times are analyzed.

D. RESULTS AND DISCUSSION

Table 11 presents the received power from the routers in the BR. The received power was calculated based on the EWMA for the RSL of each router, which is stored in the BR after measuring 14 channels in the star network. Since the nodes were connected by the evaluation board in the measurement, the received power of each node in the BR was distributed from –47 dBm to the upper limit of the measurement range of –41 dBm. All the nodes can communicate with each other with sufficient received power since the minimum received power of Wi-SUN FAN module achieves the required Packet Error Rate (PER) is –104 dBm [2].

TABLE 11. Received Power From Routers at the BR

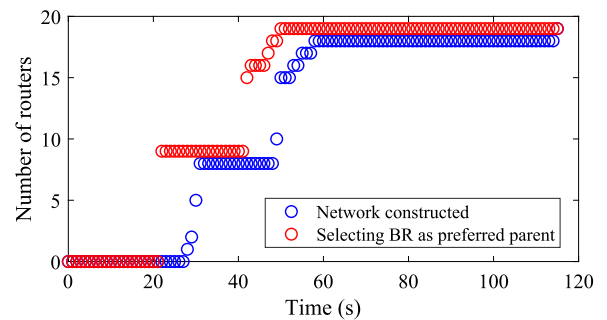| Node index	Received power (dBm)	Node index	Received power (dBm)
Router 1	–42	Router 11	–41
Router 2	–42	Router 12	–42
Router 3	–41	Router 13	–42
Router 4	–42	Router 14	–47
Router 5	–41	Router 15	–43
Router 6	–41	Router 16	–41
Router 7	–41	Router 17	–41
Router 8	–41	Router 18	–41
Router 9	–41	Router 19	–41
Router 10	–41		

FIGURE 15. Transition of the number of Router connected to BR (star topology, experiment).

First, a star topology network is analyzed. Fig. 15 presents the transition of the number of routers connected to the BR when the FH with 14 channels is used. The vertical axis represents the number of routers that joined the network and the number of routers that have selected the BR as their parent nodes. Joining the network was completed when the join state of the router was five. The number of routers was counted in intervals of 1 s. Following a period of 22 s, nine routers selected the BR as the parent node. This is because the BR transmitted the DIO and the nine routers that received it selected the BR as the parent node. Once the parent node is selected, the router transmits a DAO and completes the joining of the network when communication with the BR is confirmed. The network construction was completed within a relatively short period of 115 s in the small-scale network to be measured.

Fig. 8 presents the average transmission success rate of all nodes corresponding to the packet generation rate. The average transmission success rate was maintained at one for both cases, i.e., for 14 channels and one channel. Fig. 9 presents the average delay time characteristics of all the nodes for the packet generation rate. From both figures, the characteristics determined by the computer simulation and experimental evaluation environment were in good agreement. In the experimental results, the average delay time is approximately 0.126 s for a packet generation rate of 1.00×10^{-1} s^{-1} when 14 channels are used. This is longer than the average packet transmission processing time of 65.801 ms given in Table 5. This delay is caused by the
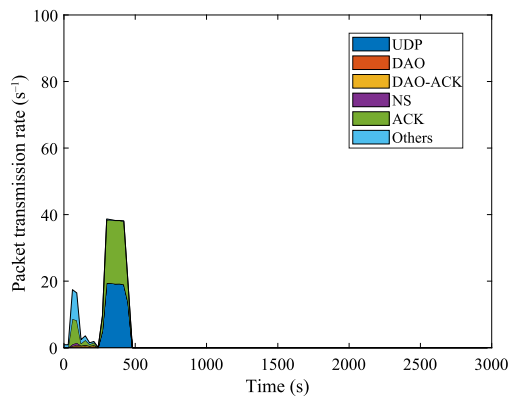
FIGURE 16. Breakdown of the number of packets transmitted per unit time when packet generation rate is 1.00 s^{-1} and the number of channels used is one (star topology, experiment).

TABLE 12. Breakdown of the Number of Total Packets Transmitted in the Period When UDP Packets are Transmitted (Star Topology, Experiment, 1 Channel)

Packet generation rate (s^{-1})	Time (s)	Packet count					
		UDP	DAO	DAO ACK	NS	ACK	Other
1.00×10^{-1}	1679.1	3182	38	38	57	3310	329
3.33×10^{-1}	575.3	3637	19	19	19	3672	103
5.00×10^{-1}	395.3	3394	0	0	3	3237	68
1.00	171.0	3279	0	0	0	3134	29

various data processing times in the actual devices. The primary delay factors in the actual device include the processing time by the input/output of commands and logs, etc. via the serial interface. It takes approximately 27.8 ms to input the 200 bytes user data and output it at the receiving end since the data rate of the serial interface of the USB board is 115200 bps. Since there are other inputs/outputs of control information, it is assumed to be one of the primary delay factors. Conversely, if the packet generation rate is 1.00 s^{-1} and only one channel is used, the average delay time is approximately 0.204 s. Fig. 16 presents a breakdown of the packet transmission rate in this case. The packets, which are present prior to the beginning of the UDP packet transmission, are the packets related to PAN construction, such as PA, PC, and packets related to security flow in IEEE 802.1X. Table 12 presents a breakdown of the number of packets transmitted in the period when UDP packets are transmitted. The total data packet generation ratio for all nodes is 19 s^{-1} after the UDP packet transmission begins; however, the UDP packet transmission rate is approximately 19.3 s^{-1} (3279 packets/171.0s), indicating that retransmissions occurred for some packets. The retransmission due to such packet collisions is a factor which increases the delay time.

Second, a tree topology network is analyzed. Fig. 17 presents the transition of the number of routers when the FH with 14 channels was considered. For five routers configured to select the BR as the parent node by MAC filtering, all selected the BR as the parent node after 223 s. The period until all routers completed their participation in the network
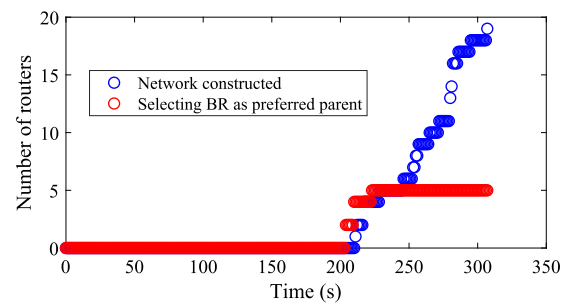

FIGURE 17. Transition of the number of Router connected to BR (tree topology, experiment).
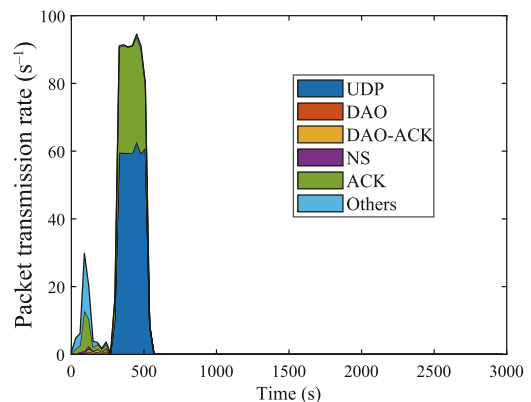

FIGURE 18. Breakdown of the number of packets transmitted per unit time when packet generation rate is 1.00 s^{-1} (tree topology, experiment, 14 channels).

TABLE 13. Breakdown of the Number of Total Packets Transmitted in the Period When UDP Packets are Transmitted (Tree Topology, Experiment,14 Channels)

Packet generation rate (s^{-1})	Time (s)	Packet count					
		UDP	DAO	DAO ACK	NS	ACK	Other
1.00×10^{-1}	1820.9	6045	106	106	59	6356	415
3.33×10^{-1}	569.6	7311	43	45	21	6427	204
5.00×10^{-1}	408.0	8082	0	0	12	6886	171
1.00	208.4	12419	0	0	0	6330	83

is 307 s. In the tree topology network evaluated in this study, once the routers that perform packet transfer join the network, the routers that perform packet transfer twice join the network. Accordingly, the period until the network construction is completed becomes longer compared to the star topology network. Fig. 11 presents the average transmission success rate of all the nodes for the specified packet generation rate. The average transmission success rate for both number of channels of 14 and 1, was approximately 1 in the range in which the packet generation rate is 5.00×10^{-1} s^{-1} or lesser. Conversely, the average transmission success rate drops significantly when the packet generation rate is 1.00 s^{-1}. It is approximately 0.86 when the number of channels used was 14 with FH. Fig. 18 presents a breakdown of the packet transmission rate in this case. Table 13 presents a breakdown of the number
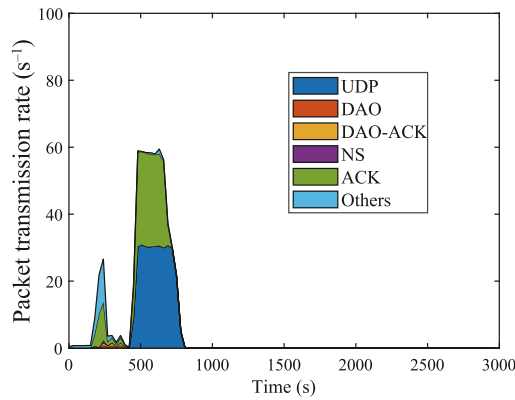
FIGURE 19. Breakdown of the number of packets transmitted per unit time when packet generation rate is 1.00 s^{-1} (tree topology, experiment, 1 channel).

TABLE 14. Breakdown of the Number of Total Packets Transmitted in the Period When UDP Packets are Transmitted (Tree Topology, Experiment, 1 Channel)

Packet generation rate (s^{-1})	Time (s)	Packet count					
		UDP	DAO	DAO ACK	NS	ACK	Other
1.00×10^{-1}	1629.9	5330	68	66	57	5548	376
3.33×10^{-1}	501.8	5553	26	22	19	5544	179
5.00×10^{-1}	372.3	5667	0	0	0	5540	157
1.00	224.8	6803	0	0	0	6096	95

of packets transmitted in the period when the UDP packets are transmitted. Since there are five routers which perform packet transfer once and 14 routers which perform packet transfer twice, the expected total UDP packet transmission rate is approximately 33 s^{-1} for all nodes when no packet retransmission occurs. Conversely, the UDP packet transmission rate shown in Fig. 18 is approximately 60.1 s^{-1} since collisions occur in many UDP packets and retransmission is performed.

The average transmission success rate is approximately 0.68 when one channel is used. Fig. 19 presents the breakdown of the packet transmission rate in this case. Table 14 presents a breakdown of the number of packets transmitted in the period when the UDP packets are transmitted. The UDP packet transmission rate during the packet transmission interval is approximately 30.3 s^{-1}, which is less than the case when 14 channels are used. This is because the number of transmitted packets is restricted by the limited number of channels. It can be observed that some UDP packets have not been received due to conflicts, etc., primarily because the ACK frame transmission rate is approximately 27.5 s^{-1}, which is less than the UDP packet transmission rate. Fig. 12 depicts the average delay time characteristics of all the nodes for packet generation rate. The average delay time is approximately 0.175 s when 14 channels are used and approximately 0.187 s when one channel is used for a packet generation rate of 1.00×10^{-1} s^{-1}. This delay time represents the actual packet transmission delay time along with various data processing times in the actual devices similar to the star topology
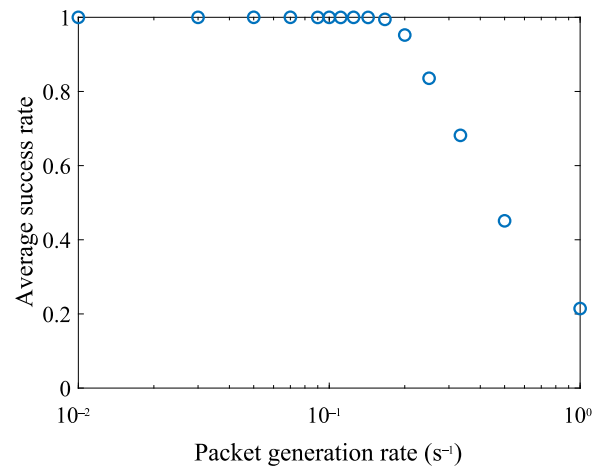

FIGURE 20. Average transmission success rate (fixed large-scale tree topology, 100 router nodes).

network. Conversely, the average delay time is approximately 0.806 s when 14 channels are in use and approximately 3.535 s when one channel is in use, and in both cases, the packet generation rate is 1.00 s^{-1}, which is a relatively high packet transmission rate (one packet per second). The significant increase in latency for 1 channel can be attributed to the backoff retries, packet retransmissions, latency in packet buffers, and limited number of channels.

In terms of the breakdown of the number of total packets, the characteristics determined by the computer simulation and experimental evaluation environment were in good agreement.

VI. PERFORMANCE ANALYSIS IN MULTIPLE LARGE-SCALE WI-SUN FAN TOPOLOGIES BY VALIDATED SIMULATOR

In this section, using computer simulations validated in Section V, we evaluate the transmission performance of a Wi-SUN FAN 1.0 in multiple large-scale topologies with 100 multi-hop transmissions, as expected in an IoT application, such as smart meters.

A. TRANSMISSION PERFORMANCE IN A FIXED TOPOLOGY

With reference to Fig. 7, a tree topology was formed using 30 nodes of Group 1 connected to BR and 70 nodes of Group 2 transmitted to BR via the nodes of Group 1. In the topology, it was presumed that the node of Group 1 is always connected to BR and the node of Group 2 can be connected to any node belonging to Group 1.

Fig. 20 presents the average success rate characteristics of all the nodes corresponding to the packet generation rate. The average transmission success was maintained at approximately 1 in the range smaller than approximately 1.50×10^{-1} s^{-1}. Moreover, Fig. 21 presents the average delay time characteristics of all the nodes for the specified packet generation rate. The delay time was maintained at
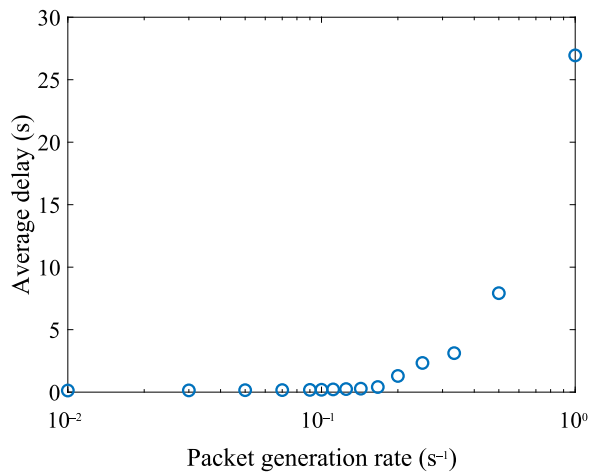
FIGURE 21. Average delay time to successfully transmit packet (fixed large-scale tree topology, 100 router nodes).
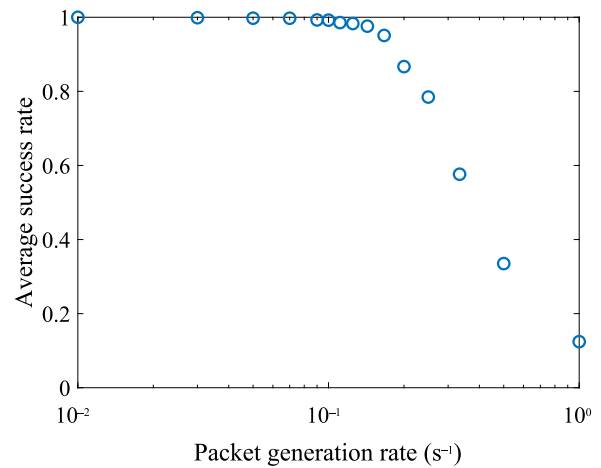

FIGURE 23. Average transmission success rate (a large-scale tree topology assuming for outdoor installation, 100 router nodes).
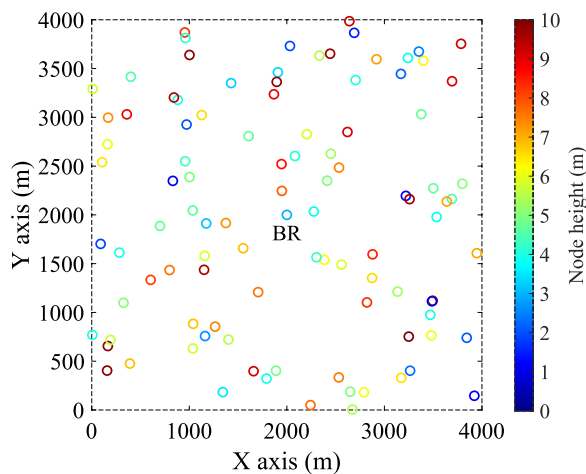

FIGURE 22. Node arrangement example used for the evaluation.
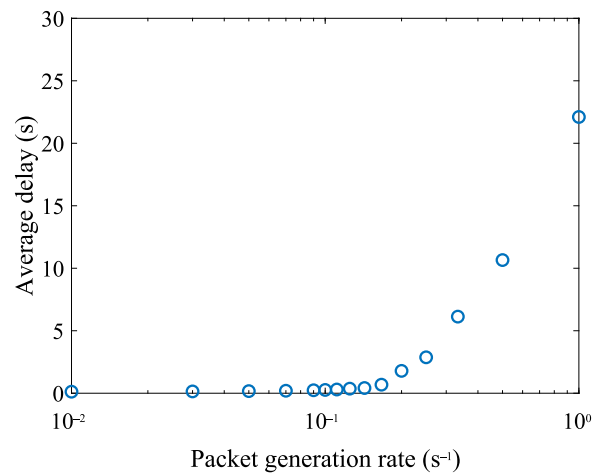

FIGURE 24. Average delay time to successfully transmit packet (a large-scale tree topology assuming for outdoor installation, 100 router nodes).

approximately zero in the range smaller than approximately 1.50×10^{-1}. Based on these results, the information generated once every 10 seconds at all nodes can be transmitted to BR even though 100 units are connected.

B. TRANSMISSION PERFORMANCE ASSUMING FOR OUTDOOR INSTALLATION

The evaluation is conducted by assuming that the IoT device with Wi-SUN FAN is installed outdoors. An example of node layout used for the evaluation is depicted in Fig. 22. One BR was placed in the center of a 4000 m square flat field, and 100 routers were randomly positioned. The height from a router to the ground is uniformly distributed from 1–10 m. The height of BR was 3 m. These installation models were referred from [15]. Moreover, with regards to route construction using RPL, a router can connect to other routers without limitation, and there is no upper limit on the number of child nodes that can connect to each router. Simulation parameters for

Wi-SUN FAN are listed in Tables 1, 2 and 3. As a model of radio propagation model between nodes, a two-ray ground reflection model [16] was adopted, similar to [15].

Fig. 23 presents the average success rate characteristics of all nodes corresponding to the packet generation rate. Same as Fig. 20, the average transmission success rate was maintained at approximately 1 in the range smaller than approximately 1.0×10^{-1} s^{-1}. Moreover, Fig. 24 presents the average delay time characteristics of all the nodes corresponding to the packet generation rate. Same as Fig. 21, the delay time was maintained at approximately zero in the range smaller than approximately 1.0×10^{-1}.

Fig. 25 illustrates an example of a finally constructed network topology. It can be observed that even when 100 nodes of router are randomly positioned in a flat square field with 4000 m on a side, the constructed tree topology is almost the same type of ones evaluated in Sections IV and VI.A, most number of hops is one same as Sections IV and VI.A and some of them
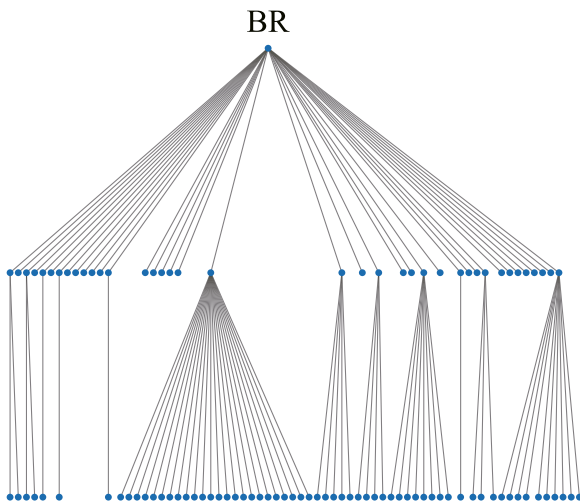
BR

FIGURE 25. Constructed route (fixed large-scale tree topology, 100 router nodes).

is two. Consequently, the fundamental evaluation of this study can be used as the reference data for performance evaluation of large-scale Wi-SUN FAN networks.

VII. CONCLUSION

In this study, evaluation environments were developed using computer simulations and actual experimental devices certified by Wi-SUN alliance on the Wi-SUN FAN 1.0 network standardized by IEEE 2857 as a wireless communication standard for IoT applications. The average transmission success rate and average delay time were evaluated. Moreover, it was confirmed that the characteristics determined by the computer simulation and the experimental evaluation environment conform with each other, and that the constructed computer simulation environment simulates the experimental environment using actual devices. Furthermore, it is demonstrated that the reference data of the Wi-SUN FAN 1.0 system can be obtained using these two evaluation environments. In this study, a network is considered with one BR and 19 routers; however, in the star topology network, the average transmission success rate is maintained at one, regardless of the communication frequency. Conversely, in the tree topology, the average transmission success rate is maintained at approximately 1 at 5.00×10^{-1} s^{-1} or less. However, when the packet generation rate is 1.00 s^{-1}, the average transmission success rate for both the computer simulation and the actual machine reduced to approximately 0.59 and 0.68, respectively. This indicates that Wi-SUN FAN 1.0 may be able to communicate with a higher transmission success rate even when transmitting frequent IoT-data, which is once every few seconds. To confirm the feasibility of Wi-SUN FAN in large-scale environment, we evaluated the transmission performance in the wireless IoT environment with one BR and 100 routers that were randomly arranged in a flat square field with 4000 m on

a side by using the validated simulator. The average transmission success rate was maintained at approximately 1 in the range less than approximately 1.0×10^{-1} s^{-1}. Consequently, Wi-SUN FAN 1.0 can communicate with a higher transmission success rate even when transmitting frequent IoT-data, which is once every ten seconds. The results in this study confirmed that Wi-SUN FAN can be effectively used for smart metering systems, which transmit data once every ten minutes, to IoT applications, which transmit data once every ten seconds. In summary, Wi-SUN FAN will drive next-generation wireless IoT communication. Future research objectives include computer simulation-based evaluation and experimental evaluation using hundreds of actual Wi-SUN FAN devices in various applications. Moreover, although transmission characteristics of Wi-SUN FAN under stable conditions were evaluated assuming smart meters in this study, it will be necessary in the future to discuss the effectiveness of the RPL protocol standardized in Wi-SUN FAN, taking into account the dynamic topology constructed by RPL.

REFERENCES

[1] U. Raza, P. Kulkarni, and M. Sooriyabandara, "Low power wide area networks: An overview," *IEEE Commun. Surveys Tuts.*, vol. 19, no. 2, pp. 855–873, Second Quarter 2017.
[2] H. Harada, K. Mizutani, J. Fujiwara, K. Mochizuki, and K. Obata, "IEEE 802.15.4g based Wi-SUN communication systems," *IEICE Trans. Commun.*, vol. E100-B, no. 7, pp. 1032–1043, Jul. 2017.
[3] T. Junjalearnvong, R. Okumura, K. Mizutani, and H. Harada, "Performance evaluation of multi-hop network configuration for Wi-SUN FAN systems," in *Proc. IEEE 16th Annu. Consum. Commun. Netw. Conf.*, 2019, pp. 1–6.
[4] K. Mizutani, R. Okumura, K. Mizutani, and H. Harada, "Coexistence of synchronous and asynchronous MAC protocols for wireless IoT systems in sub-gigaherz band," in *Proc. IEEE 6th World Forum Internet Things*, 2020, pp. 1–6.
[5] D. Hotta, R. Okumura, K. Mizutani, and H. Harada, "Stabilization of multi-hop routing construction in Wi-SUN FAN systems," in *Proc. IEEE 17th Annu. Consum. Commun. Netw. Conf.*, 2020, pp. 1–6.
[6] R. Wayong, R. Okumura, K. Mizutani, and H. Harada, "A scheduling scheme for channel hopping in Wi-Sun FAN systems toward data throughput enhancement," in *Proc. IEEE 91st Veh. Technol. Conf.*, 2020, pp. 1–5.
[7] Wi-SUN alliance, "Wi-SUN alliance," 2012. [Online]. Available: https://www.wi-sun.org
[8] *IEEE Standard for Low-Rate Wireless Networks*, IEEE Standard 802.15.4-2015, IEEE, NJ, USA, Apr. 2016.
[9] "Application of advanced technology for stable operation of smart meter communication system," *TOSHIBA Rev. Sci. Technol. Highlights*, vol. 31, Mar. 2019, Art. no. 36.
[10] *IEEE Standard for Wireless Smart Utility Network Field Area Network (FAN)*, IEEE Standard 2857-2021, IEEE, NJ, USA, Jun. 2021.
[11] T. Winter et al., "RPL: IPv6 routing protocol for low-power and lossy networks," IETF RFC, Wilmington, DE, USA, Tech. Rep. 6550, Mar. 2012.
[12] P. Levis, T. Clausen, J. Hui, O. Gnawali, and J. Ko, "The trickle algorithm," IETF RFC, Wilmington, DE, USA, Tech. Rep. 6206, Mar. 2011.
[13] O. Gnawali and P. Levis, "The minimum rank with hysteresis objective function," IETF RFC, Wilmington, DE, USA, Tech. Rep. 6719, Sep. 2012.
[14] H. Harada and R. Prasad, *Simulation and Software Radio For Mobile Communications*. Norwood, MA, USA: Artech House, 2002.
[15] R. Hirakawa, R. Okumura, K. Mizutani, and H. Harada, "A novel routing method with load-balancing in Wi-SUN FAN network," in *Proc. IEEE 7th World Forum Internet Things*, 2021, pp. 362–367.
[16] A. Goldsmith, *Wireless Communications*. Cambridge, U.K.: Cambridge Univ. Press, Aug. 2005.

REI HIRAKAWA received the B.E. degree in electric and electrical engineering from Kyoto University, Kyoto, Japan, in 2020, and the M.I. degree from the Graduate School of Informatics, Kyoto University, in 2022. He researched low power and lossy network protocols for wireless smart ubiquitous networks (Wi-SUN) with Kyoto University.

KEIICHI MIZUTANI (Member, IEEE) received the B.E. degree in electric, electrical and system engineering from Osaka Prefecture University, Sakai, Japan, in 2007, and the M.E. and Ph.D. degrees in electric and electrical engineering from the Tokyo Institute of Technology, Tokyo, Japan, in 2009 and 2012, respectively. He is currently an Associate Professor of Kyoto University, Kyoto, Japan. In 2010, he was an invited Researcher with Fraunhofer Heinrich Hertz Institute, Germany. From 2012 to 2014, he was a Researcher with the National Institute of Information and Communications Technology. He is currently researches the topics of physical layer technologies in white space communications, dynamic spectrum access, wireless smart utility networks (Wi-SUN), and 4G/5G/6G systems, including OFDM, OFDMA, MIMO, and multi-hop relay network systems. Since joining in NICT, he has been involved in IEEE 802 standardization activities, namely 802.11af, 802.15.4m, and 802.22b. He was the recipient of the Special Technical Awards from IEICE SR technical committee in 2009 and 2017, Best Paper Award from IEICE SR technical committee in 2010 and 2020, Young Researcher's Award from IEICE SRW technical committee in 2016, Best Paper Award from WPMC2017 and WPMC2020, and Best Paper Presentation Award (1st Place) from IEEE WF-IoT 2020.

HIROSHI HARADA (Senior Member, IEEE) is currently a Professor of the Graduate School of Informatics, Kyoto University, and an Executive Research Director of the Wireless Networks Research Center, National Institute of Information and Communications Technology (NICT). In 1995, he joined the Communications Research Laboratory, Ministry of Posts and Communications, (currently, NICT). Since 1995, he has researched software radio, cognitive radio, dynamic spectrum access network, wireless smart ubiquitous network (Wi-SUN), and broadband wireless access systems. He also has joined many standardization committees and forums in the United States and in Japan and fulfilled important roles for them, especially IEEE 1900 and IEEE 802. He was the Chair of IEEE DySpan Standards Committee and the Vice Chair of IEEE 802.15.4g, IEEE 802.15.4m, IEEE 1900.4, and TIA TR-51. He was a board of directors of IEEE communication society standards board, SDR forum, DSA alliance, and WhiteSpace alliance. He is a Cofounder of Wi-SUN alliance and was the Chairman of the board from 2012 to 2019. He is currently the Vice Chair of IEEE 2857, IEEE 802.15.4aa, and Wi-SUN alliance. He moreover was the Chair of the IEICE Technical Committee on Software Radio and the Chair of Public Broadband Mobile Communication Development Committee, ARIB. He is also involved in many other activities related to telecommunications. He has authored the book entitled Simulation and Software Radio for Mobile Communications (Artech House, 2002). He was the recipient of the achievement awards in 2006 and 2018 and Fellow of IEICE in 2009, respectively and the achievement awards of ARIB in 2009 and 2018, respectively, on the topic of research and development on software radio, cognitive radio, and Wi-SUN.